MOLECULAR
METABOLISM

A comprehensive lipidomic screen of pancreatic β-cells using mass spectroscopy defines novel features of glucose-stimulated turnover of neutral lipids, sphingolipids and plasmalogens

Gemma L. Pearson [1,2,4,5], Natalie Mellett [3,4], Kwan Yi Chu [1], Ebru Boslem [1,2], Peter J. Meikle [3,6,**], Trevor J. Biden [1,2,6,*]

ABSTRACT

Objective: Glucose promotes lipid remodelling in pancreatic β-cells, and this is thought to contribute to the regulation of insulin secretion, but the metabolic pathways and potential signalling intermediates have not been fully elaborated.
Methods: Using mass spectrometry (MS) we quantified changes in approximately 300 lipid metabolites in MIN6 β-cells and isolated mouse islets following 1 h stimulation with glucose. Flux through sphingolipid pathways was also assessed in ^{3}H-sphinganine-labelled cells using TLC.
Results: Glucose specifically activates the conversion of triacylglycerol (TAG) to diacylglycerol (DAG). This leads indirectly to the formation of 18:1 monoacylglycerol (MAG), via degradation of saturated/monounsaturated DAG species, such as 16:0_18:1 DAG, which are the most abundant, immediate products of glucose-stimulated TAG hydrolysis. However, 16:0-containing, di-saturated DAG species are a better direct marker of TAG hydrolysis since, unlike the 18:1-containing DAGs, they are predominately formed via this route. Using multiple reaction monitoring, we confirmed that in islets under basal conditions, 18:1 MAG is the most abundant species. We further demonstrated a novel site of glucose to enhance the conversion of ceramide to sphingomyelin (SM) and galactosylceramide (GalCer). Flux and product:precursor analyses suggest regulation of the enzyme SM synthase, which would constitute a separate mechanism for localized generation of DAG in response to glucose. Phosphatidylcholine (PC) plasmalogen (P) species, specifically those containing 20:4, 22:5 and 22:6 side chains, were also diminished in the presence of glucose, whereas the more abundant phosphatidylethanolamine plasmalogens were unchanged.
Conclusion: Our results highlight 18:1 MAG, GalCer, PC(P) and DAG/SM as potential contributors to metabolic stimulus-secretion coupling.

1. INTRODUCTION

Whole-body fuel homeostasis is critically dependent on the stimulation of insulin secretion from pancreatic β-cells following the rise in blood glucose that accompanies feeding. The cellular mechanisms underlying glucose-stimulated insulin secretion (GSIS) depend absolutely on the generation of ATP [1], but additional effects of glucose on other small molecule intermediates have been recently identified using metabolomic profiling [2—4]. Notwithstanding the key role of glucose in stimulus-secretion coupling, lipid actually constitutes the predominant metabolic fuel for β-cells in the non-fed state [5]. As expected, however, fatty acid (FA) oxidation is inhibited when glucose becomes elevated, and there is an accompanying switch toward de novo synthesis with the esterification of FA side-chains onto glycerol to form

[1]Diabetes and Metabolism Division, Garvan Institute of Medical Research, 384 Victoria St, Darlinghurst, NSW, 2010, Australia [2]St. Vincent's Clinical School, Faculty of Medicine, University of New South Wales, Australia [3]Baker IDI Heart and Diabetes Institute, Melbourne, Australia

[4] Gemma Pearson and Natalie Mellett contributed equally to this project.
[5] Current address: Brehm Diabetes Research Center, University of Michigan Medical School, 1000 Wall St, Ann Arbor, Michigan, 48105-1912, USA.
[6] Peter Meikle and Trevor Biden contributed equally to this project.

*Corresponding author. Garvan Institute of Medical Research, 384 Victoria St, Darlinghurst, NSW, 2010, Australia. Tel.: +61 2 9295 8204. E-mail: t.biden@garvan.org.au (T.J. Biden).

**Corresponding author. Baker IDI Heart and Diabetes Institute, PO Box 6492, Melbourne, Vic 3004, Australia. Tel.: +61 3 8532 1770. E-mail: peter.meikle@bakeridi.edu.au (P.J. Meikle).

diacylglycerol (DAG) and triacylglycerol (TAG) [6—8]. More surprisingly, glucose also promotes the lipolysis of these lipid stores [9,10], with the net result being the dynamic cycling of FA into and out of TAG. This makes little sense from the sole perspective of nutrient utilization but has been proposed to constitute another means for regulating insulin secretion [11—13].

Despite the potential importance of TAG/FA cycling in β-cells, our understanding of both its basic biochemistry, and the signalling interface with insulin secretion remains rudimentary. The activation of neutral lipases plays a key role since GSIS is inhibited both by pan-lipase inhibitors such as Orlistat [9,14] and by deletion of hormone-sensitive lipase (HSL) [10,15,16] and adipose tissue glycerolipase (ATGL) [17]. However, these findings require re-evaluation following a more complete characterization of these two lipases in other cell types, where ATGL acts predominately on TAG to generate DAG, which is then further degraded to MAG by HSL [18,19]. The latter also hydrolyses cholesterol ester (CE) to free cholesterol (COH). All these esterified lipids can also be degraded by lysosomal acid lipase, via the process of lipophagy [20], which we have recently shown serves as a chronic, negative regulator of GSIS [21]. How glucose interacts in these metabolic pathways is important for identifying intermediates that regulate secretion over the short, and potentially longer, term.

In addition to hydrolytic pathways, glucose can also remodel neutral lipid pools via de novo synthesis [6,8,22,23]. Phospholipid hydrolysis constitutes yet another route for generating DAG, especially species containing arachidonic acid (C20:4), which are much better characterized as signalling mediators. These species are enhanced in β-cells not only via classic receptor-dependent mechanism, but also in response to glucose [22,23]. This is mediated via a Ca^{2+}-dependent activation of two phospholipases: phospholipase C [24], acting on derivatives of phosphatidylinositol (PI); and phospholipase D [25], which hydrolyses predominately phosphatidylcholine (PC) or phosphatidylethanolamine (PE). Yet another potential route for the generation of DAG arises from the action of sphingomyelin synthase (SMS), which catalyses the condensation of ceramide with PC, to form DAG plus SM. Although this enzyme plays an essential but poorly described function in the distal secretory pathway of β-cells [26,27], its contribution in the context of lipid metabolism has not been addressed. Phospholipid remodelling also occurs in response to the activation by glucose of phospholipase A2 (PLA2), giving rise to lyso-phospholipid species and free FAs, predominately arachidonic acid, which is implicated in the regulation of insulin secretion [28]. There is evidence that the preferred substrates in β-cells of this PLA2 are plasmalogens, phospholipids in which the FA side-chain in the sn-1 position is attached by a vinyl ether linkage, rather than by esterification as is more common [29].

Here we have applied MS to conduct the first comprehensive and unbiased characterization of how glucose acutely regulates the turnover of phospholipids, sphingolipids and neutral lipids in β-cells. Our results point to remodelling of all three lipid classes in response to glucose, which impacts in varying ways on the overall accumulation of separate DAG and MAG species, as well PC plasmalogens and various sphingolipid metabolites. These findings shed new light on metabolic stimulus-secretion coupling in β-cells.

2. MATERIALS AND METHODS

2.1. Reagents
All tissue culture media, supplements and trypsin for MIN6 cells and isolated islets were from Thermo Fisher Scientific Australia (Scoresby, VIC, Australia). Insulin RIA kits were from Linco/Millipore (Billerica, MA).

DMSO, fatty acid free fraction V BSA, palmitate disodium salt, Orlistat, all neutral lipid standards, TLC plates, and ʟ-glucose, were from Sigma—Aldrich (St. Louis, MO). The BCA (bicinchoninic acid assay) protein assay kit was from Pierce (Rockford, IL). Organic solvents were from Thermo Fisher. ^{3}H-sphinganine was from American Radiolabelled Chemicals (St Louis MO).

2.2. Cell culture and islet isolation
The pancreatic beta cell line MIN6 was used at passages between 26 and 35, as previously described [30]. Cells were grown at 37 °C and 5% CO_2 in DMEM (25 mM glucose), supplemented with 10% FCS, 10 mM HEPES, 50 units/ml of penicillin and 50 μg/ml streptomycin. Cells were seeded 4×10^5 cells per well in 12-well plates, or at 2×10^6 in 6-well plates. Islets were isolated from male C57Bl6 mice as previously described [21]. After pancreatic digestion, islets were purified and incubated overnight in RPMI 1640 media (Roswell Park Memorial Institute 1640; 11 mM glucose) supplemented with 10% FCS, 0.2 mM glutamine, 10 mM HEPES, 50 U/ml of penicillin and 50 μg/ml streptomycin.

2.3. Glucose stimulation assays
MIN6 cells or groups of approximately 100 islets were preincubated for 1 h in Kreb's Ringer HEPES buffer (KRHB) containing 0.1% (wt/vol) BSA and 2 mM glucose (plus or minus 0.2 mM Orlistat, depending on experiment). They were then incubated for 1 h at 37 °C with KRHB containing either 2- or 20 mM glucose (plus or minus Orlistat, depending on experiment). An aliquot of the buffer was taken, and insulin release measured by RIA.

2.4. Lipidomic profiling using MS
Following treatment and glucose stimulation, islets (100 or 200 islets per condition) or MIN6 cells (2 wells of a 6-well plate per condition) were pelleted in ice cold PBS. Samples were extracted and analysed as previously described [31]. Briefly, cells were subjected to a single phase extraction using an addition of 20 times volume of chloroform:methanol 2:1, followed by sonication and centrifugation to pellet any protein precipitate. The supernatant was removed and dried under vacuum before the samples were reconstituted in equal volumes of water saturated butanol and 10 mM ammonium formate in methanol. Samples were run through an Agilent 1200 HPLC, with an Agilent 2.1×50 mm C18 column, coupled to an AB SCIEX Qtrap 4000 mass spectrometer and subjected to lipidomic analysis of TAG, DAG, sphingolipids and phospholipids as previously described [30,32,33]. For analysis of MAG species, 50 pmol of MAG 17:0 (Avanti Polar Lipids, Alabaster, AL) was added to each sample as an internal standard, prior to lipid extraction. We used the same equipment as above with the following voltages: collision energy (15 V); declustering potential (76 V); and exit potential (16 V). MAG species were then monitored during the chromatographic elution [33] and quantified by comparing peak areas relative to that of the internal standard. For multiple reaction monitoring [31], individual MAG species were identified from a combination of neutral loss scans and literature data. The neutral loss scan is based on the loss of glycerol (92 Da) across a mass range of 300—600 Da.

2.5. Radiolabelling and TLC
MIN6 cells were seeded in 12-well plates followed by glucose stimulation in KRBH in the presence of 5 μCi/ml of ^{3}H-sphinganine for 1 h. Cells were washed with cold PBS, gently lysed in 0.1% SDS in PBS, and an aliquot of sample taken for protein quantification, by BCA assay. Total lipid was then extracted by addition of chloroform:methanol [2:1 (v/v)] solution, followed by washing with milli-Q water. The organic
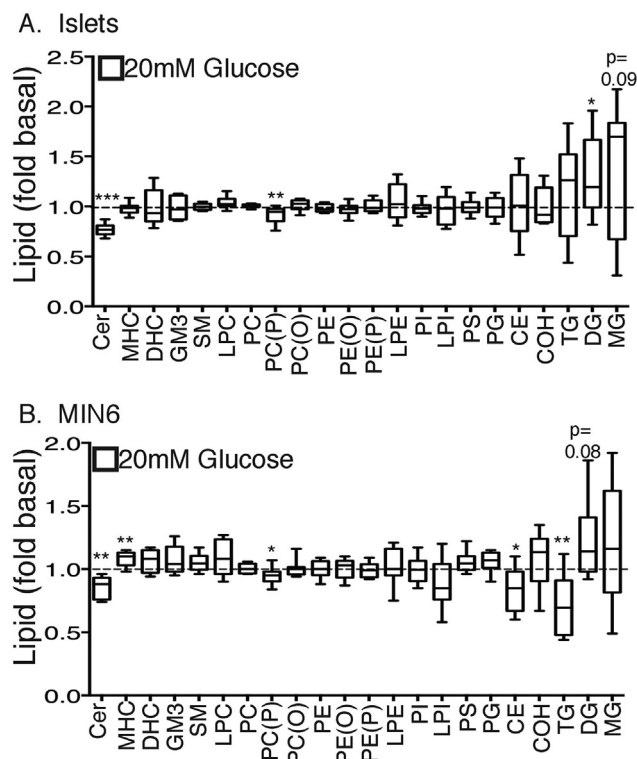
A. Islets

B. MIN6

Figure 1: Alterations in total content of major lipids following glucose stimulation in MIN6 cells and primary islets. Isolated islets (A) and MIN6 cells (B) were stimulated with either 2- or 20 mM glucose for 1 h. Cellular lipids were extracted and then subjected to MS, as per Methods. For each lipid class reported, all measured species were summed, and normalized to total phospholipid content. Results are expressed as a fold change of 20 mM glucose to 2 mM glucose. *$p < 0.05$, **$p < 0.01$, ***$p < 0.001$ Student's unpaired t-test, corrected for multiple comparisons (Holm Sidak). n $= 7-9$ experiments (A) or n $= 6-8$ experiments (B). Abbreviations as per text plus: Cer, ceramide; DHC, dihexosylceramide; GM3, monosialodihexosylganglioside; LPI, lyso-PI; PS, phosphatidylserine; PG, phosphatidylglycerol.

phase was then dried down under N_2, and resuspended in 25 μL chloroform:methanol [2:1 (v/v)]. These samples, supplemented with unlabelled standards, were then run on acetone-activated TLC chloroform:methanol:water [65:25:4, by vol.] for analysis of sphingolipids [34]. The plate was then exposed to Kodak MR film for 6 days at $-80\ ^\circ$C. Following development of the film, the plate was iodinated overnight, to visualise the lipid standards, and spots of interest were scraped, combined with 5 mL scintillation fluid and counted on a β-counter (Beckman Coulter, S6000SC).

2.6. Statistical analysis

All data are expressed as mean $\pm$ S.E.M. All statistics were performed using GraphPad Prism5 software (GraphPad software, La Jolla, USA) and subjected to either: one-way ANOVA (with Sidak's post-test); two-way ANOVA (with Sidak's multiple comparison post-test); or Student's unpaired t-test, (corrected for multiple comparisons according to Holm Sidak).

3. RESULTS

3.1. Lipid turnover in islets and MIN6 cells

We conducted a comprehensive lipidomic screen of both isolated mouse islets and MIN6 cells to investigate changes following 1 h

stimulation with glucose. This entailed analysis of more than 350 individual species, comprising more than a dozen major lipid classes and including members of each of the phospholipid, sphingolipid and neutral lipid families. The full list of the 300 metabolites that were consistently detected in mouse islets is provided in Supplementary Table 1. Very few of the changes due to glucose, however, maintained statistical significance after correction for multiple analyses. Nevertheless, responses in ceramides, disaturated DAG species and PC(P) plasmalogens were sufficiently noteworthy to prompt further investigation. As an additional screening approach we have summed all the species for each major lipid class, to obtain a measure of its total mass, and determined the response of 20 mM glucose expressed relative to basal (2 mM glucose). There was generally very good agreement between results obtained with islets (Figure 1A) and those in MIN6 cells (Figure 1B). A major exception was cholesterol metabolism, with a possible remodelling of CE to COH due to glucose that was more pronounced in MIN6 cells than islets. Although glucose stimulation barely altered the total content of any of the major phospholipid classes of PC, PE, PI, or phosphatidylserine, the PC plasmalogen (P) was decreased in both models. This was highly specific, as it was not observed in PC ether lipids (PC(O)), containing non-vinyl ether linkages in the sn-1 position. Nor were the PE plasmalogens (PE(P)) or ether lipids (PE(O)) altered. The most obvious effect of glucose on sphingolipid metabolism was a highly significant decrease in ceramide, accompanied in MIN6 cells only by an increase in the glycosylation product monohexosylceramide (MHC). Of the neutral lipid class, TAG was diminished in MIN6 cells in response to glucose (Figure 1B), and there was a clear trend toward increases in DAG (significantly so in islets) and less obviously in MAG.

3.2. DAG metabolism in response to glucose

DAG was chosen initially for more detailed analysis of the changes in individual species. These results are normalized to phospholipid content for islets, which did not vary between high and low glucose treatments (102 ± 5 versus 105 ± 12 nmol/mg protein). The greater availability and reproducibility of MIN6 cells allowed us to present results as mass per unit protein for these individual DAG species, with good concordance between the two datasets (Figure 2). We observed different regulatory patterns depending on whether the FA side-chains were di-unsaturated; mixed saturated and unsaturated; or contained arachidonic acid (C20:4). The capacity of glucose to stimulate DAG was most obvious in the di-saturated group in both islets (Figure 2A) and MIN6 cells (Figure 2D), with significant effects of glucose observed both for individual species, and across all di-saturated species by 2-way ANOVA ($p = 0.004$ for islets and $p = 0.01$ for MIN6 cells respectively). Little overall change was observed in the 20:4-containing species (Figure 2C,F), although the modest decrease in 18:1_20:4 DAG in islets was statistically significant. Mixed species showed an intermediate response, with a tendency for only the most abundant representative (16:0_18:1 DAG) to be augmented (Figure 2B,E).

To address the source of these DAG increases, we next examined the impact of Orlistat, a general inhibitor of neutral lipases. When added during the 1 h glucose stimulation of MIN6 cells, this inhibited insulin secretion (Figure 3A). It also enhanced the overall accumulation of TAG (Figure 3B) and diminished that of MAG (Figure 3D). Basal DAG was not altered under these conditions (Figure 3C), probably due to competing inhibitory effects on both its generation from TAG, and its breakdown to MAG. Notably, however, Orlistat completely abolished the accumulation of DAG in response to glucose (Figure 3C). This was confirmed when the 16:0_16:0 DAG (Figure 4A) and 16:0_18:1DAG species (Figure 4B) were examined as representative of the di-saturated and
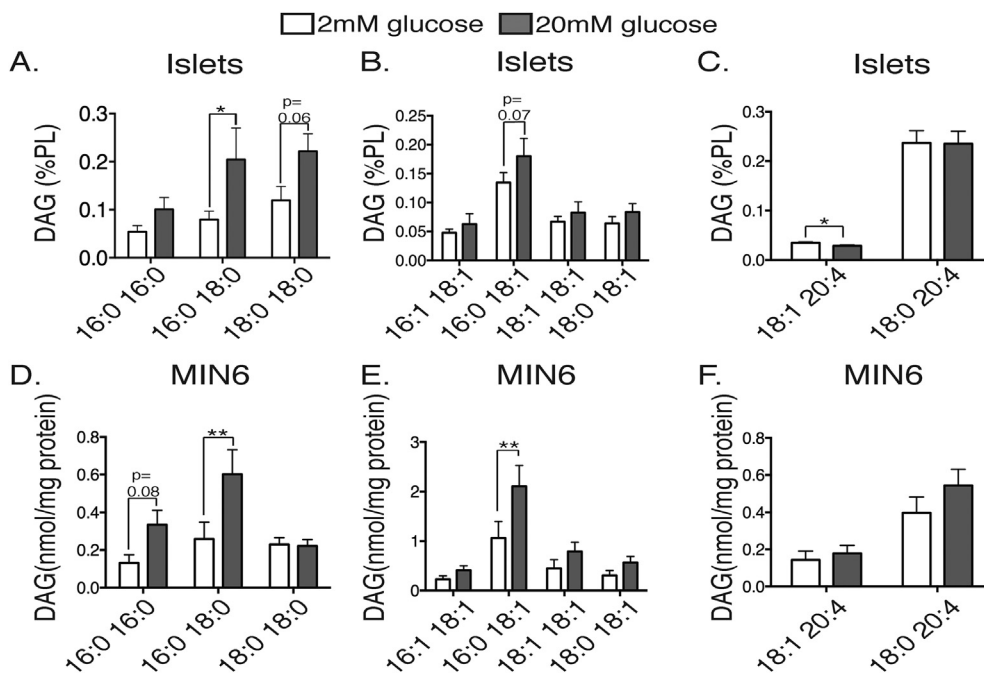
Figure 2: Glucose preferentially increases C16:0-containing, di-saturated DAG species in primary islets (A–C) and MIN6 cells (D–E). Cellular lipids were extracted and then subjected to MS, as per Methods. Results are presented as mass normalized to total phospholipid content (A–C) or protein content (D–E) following stimulation with 2 mM (white bars) or 20 mM glucose (grey bars) for 1 h. DAG species are grouped as containing side chains that are di-saturated (A,D), mixed (B,E) or containing C20:4 (C,F). *p < 0.05, **p < 0.01, Student's unpaired t-test assuming similar scatter in these populations, and corrected for multiple comparisons (Holm Sidak). n = 7−9 experiments (A) or n = 6−7 experiments (B).
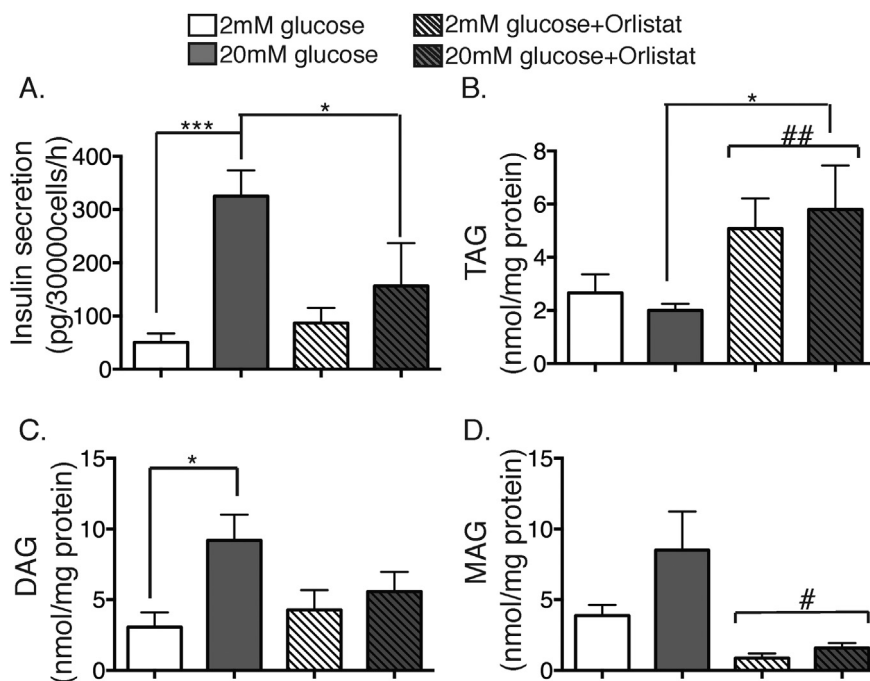

Figure 3: Inhibition of neutral lipolysis increases TAG, decreases MAG and inhibits the generation of DAG by glucose. MIN6 cells were stimulated with either 2 mM (white bars), or 20 mM glucose (grey bars) or 2 mM (white striped bars) or 20 mM glucose + 0.2 mM Orlistat (grey striped bars) for 1 h. (A) GSIS was measured by RIA. (B−C) Total cellular lipids were extracted and then subjected to MS, as per Methods. (B) total TAG, (C) total DAG, and (D) total MAG. *p < 0.05, ***p < 0.001, one-way ANOVA, Sidak's post-test; #p < 0.05; ##p < 0.01 two-way ANOVA for effect of Orlistat. n = 3−6 experiments.
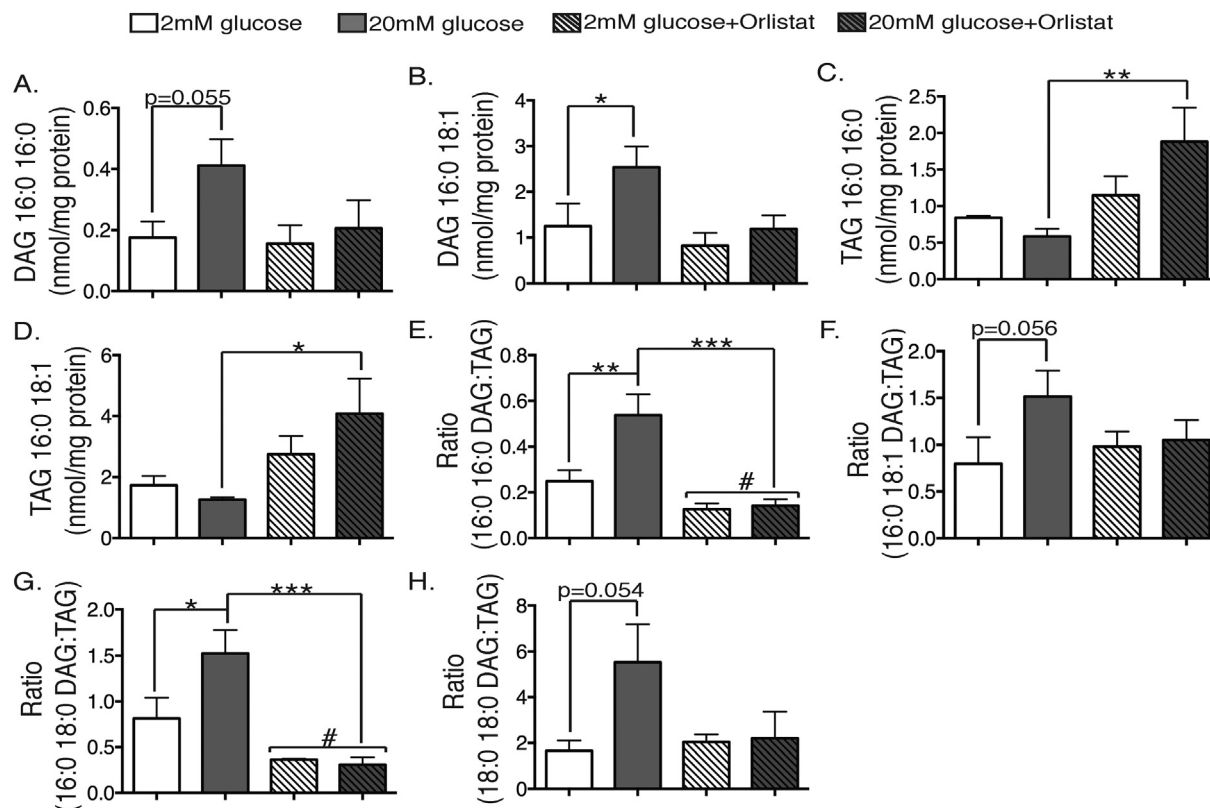
Figure 4: C16:0-containing, di-saturated DAG species reflect TAG hydrolysis after glucose stimulation in β-cells. MIN6 cells were stimulated with either 2 mM (white bars), or 20 mM glucose (grey bars) or 2 mM (white striped bars) or 20 mM glucose + 0.2 mM Orlistat (grey striped bars) for 1 h. Total cellular lipids were extracted and then subjected to MS, as per Methods for quantification. (A) 16:0_16:0 DAG, (B) 16:0_18:1 DAG, (C) total TAG containing two C16:0 side-chains, (D) total TAG containing both C16:0 and C18:1 side-chains, (E) ratio 16:0_16:0 DAG to all 16:0_16:0-containing TAG species, (F) ratio of 16:0_18:1 DAG to all 16:0 18:1-containing TAG species, G) ratio of 16:0 18:0 DAG to all 16:0 18:0-containing TAG species, H) ratio of 18:0 18:0 DAG to all 18:0 18:0-containing TAG species. *$p < 0.05$, **$p < 0.01$, ***$p < 0.001$ one-way ANOVA, Sidak's post-test; #$p < 0.05$ two-way ANOVA for effect of Orlistat. $n = 4-6$ experiments.

mixed groups respectively. These results suggest that the glucose-stimulated generation of these DAG species is chiefly secondary to the activation of TAG hydrolysis by a neutral lipase such as ATGL. We therefore searched for corresponding changes in the putative, precursor pools of TAG, namely those species containing either two C16:0 chains (Figure 4C) or both a C16:0 and C18:1 chain (Figure 4D). Although decrements due to glucose stimulation failed to reach statistical significance, they were of sufficient magnitude to account, at least potentially, for the accompanying increases in DAG. We therefore re-analysed these data as product-precursor ratios by directly calculating the ratio of 16:0_16:0 DAG to the corresponding TAG pool under all treatment conditions (Figure 4E). Orlistat strongly reduced this ratio independently of glucose but also specifically abolished the increase due to glucose. When the corresponding analysis was applied to the 16:0_18:1 DAG:TAG ratio, however, the effects of both glucose stimulation and Orlistat pretreatment were less pronounced (Figure 4F). These results suggest some fundamental differences: 16:0_16:0 DAG is predominately generated by TAG hydrolysis under both basal and stimulated conditions; other routes (perhaps de novo synthesis) contribute to the basal accumulation of 16:0_18:1 DAG, but the increment due to glucose, which is quite large quantitatively (Figure 4B), is derived from breakdown of TAG. We further analysed the other two di-saturated DAG species suggested above (Figure 2) to be glucose-sensitive. 16:0_18:0 DAG (Figure 4G) gave results very similar to those of 16:0_16:0 DAG, whereas 18:0_18:0 DAG (Figure 4H) was

more akin to 16:0_18:1 DAG. We therefore propose that the C16:0-containing, di-saturated DAGs are good markers for TAG hydrolysis, even if they probably represent only a very small proportion of the overall DAG liberated by this route, especially during glucose stimulation where other abundant pools of TAG are also mobilized.

A different pattern was observed for the 20:4-containing DAG species. The most obvious effect was that of Orlistat, which acted independently of glucose to augment the abundance of both 18:1_20:4 DAG (Figure 5A) and 18:0_20:4 DAG (Figure 5B), and conversely to diminish accumulation of their breakdown product, 20:4 MAG (Figure 5C). Indeed, a clear product-precursor relationship was established from the ratio of 20:4 MAG to total 20:4-containing DAG species, which was unaltered by glucose stimulation but virtually abolished by Orlistat (Figure 5D). This would implicate a neutral lipase (such as DAG lipase) in the degradation, but not in the formation, of 20:4-containing DAG species in β-cells.

3.3. Glucose-stimulated MAG metabolism
We next turned to a broader analysis of MAG species. In both islets (Supplementary Table 1) and MIN6 cells (Figure 6A), 18:1 MAG was the most abundant species. It was augmented by glucose stimulation in the MIN6 model (Figure 6A), with a similar but non-significant trend observed in islets (Supplementary Table 1). This increase was markedly sensitive to Orlistat (Figure 6B), as would be consistent with a mode of generation requiring two neutral lipases, namely the
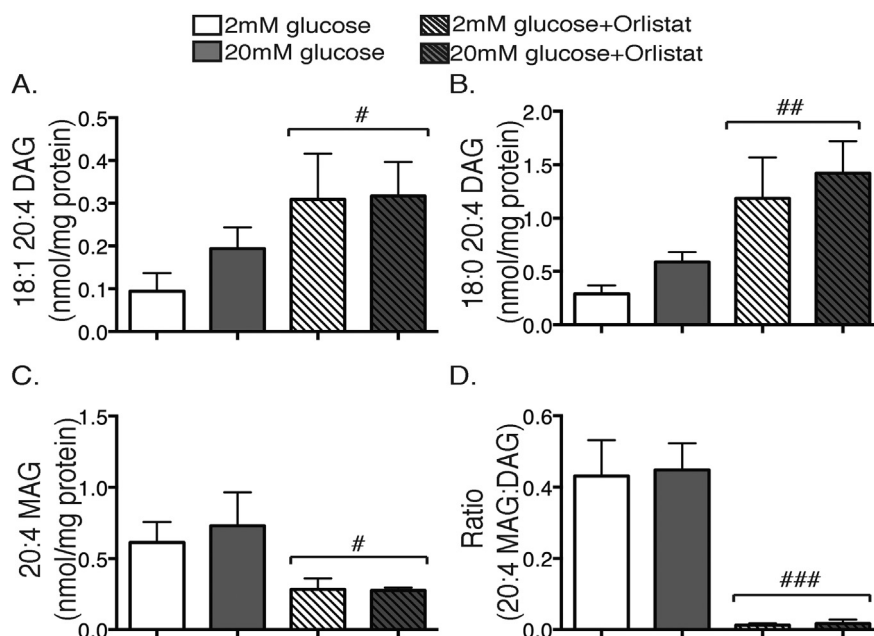
Figure 5: 20:4-containing DAG species are degraded by a neutral lipase in β-cells. MIN6 cells were stimulated with either 2 mM (white bars), or 20 mM glucose (grey bars) or 2 mM (white striped bars) or 20 mM glucose + 0.2 mM Orlistat (grey striped bars) for 1 h. Total cellular lipids were extracted and then subjected to MS, as per Methods. (A) 18:1_20:4 DAG, (B) 18:0_20:4 DAG, (C) 20:4 MAG, (D) ratio of 20:4 MAG to all 20:4-containing DAG species. #p < 0.05, ##p < 0.01, ###p < 0.0005 two-way ANOVA effect of Orlistat. n = 3–6 experiments.
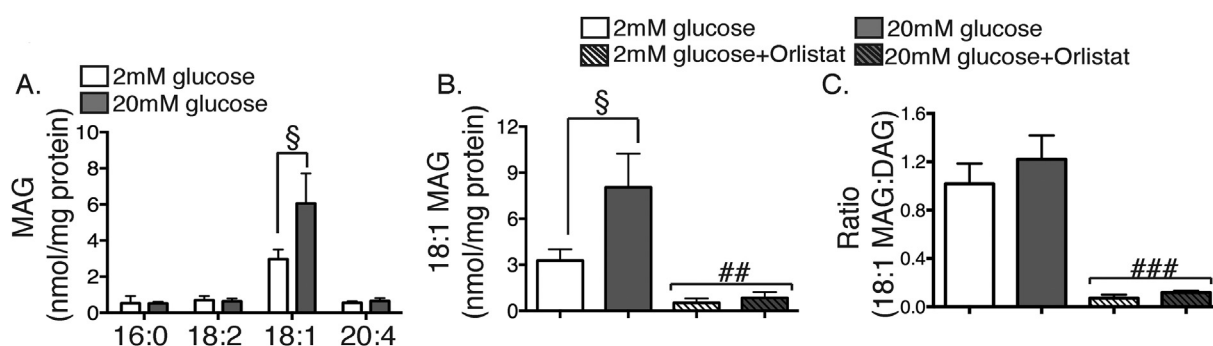

Figure 6: Generation of 18:1 MAG by glucose is secondary to TAG hydrolysis. MIN6 cells were stimulated with either 2 mM (white bars), or 20 mM glucose (grey bars) or 2 mM (white striped bars) or 20 mM glucose + 0.2 mM Orlistat (grey striped bars) for 1 h. Total cellular lipids were extracted and then subjected to MS, as per Methods. (A) major MAG species, (B) 18:1 MAG, (C) ratio of 18:1 MAG to all 18:1 containing-DAG species. §p < 0.05 two-way ANOVA corrected for multiple comparisons (Holm Sidak); ##p < 0.01, ###p < 0.005 two-way ANOVA for effect of Orlistat. n = 3–6 experiments.

conversion of TAG to DAG, and then DAG to MAG. Indeed, the ratio of 18:1 MAG to 18:1-containing DAG species was greatly reduced by Orlistat (Figure 6C). Note, however, that this ratio was not altered by glucose (Figure 6C), unlike that for DAG:TAG (Figure 4). This suggests that glucose regulates flux through the overall pathway via activation of TAG hydrolysis rather than by regulating the conversion of DAG to MAG. These findings are broadly supportive of recent work pointing to a role for MAG in regulating GSIS, although 18:1 MAG was not reported as an abundant species in those studies [35,36]. To further investigate this discrepancy, we undertook a second baseline assessment of islet MAG isoforms using double the starting material (around 200 islets/replicate) of those above and employing literature sources and neutral loss scans to identify all potential MAG species that were present. This separate cohort (Supplementary Table 2) confirmed that, of the 22 MAG species examined, only 5 accounted for >95% of total MAG, with

18:1 MAG predominating over the species containing saturated C16:0 or C18:0 side-chains.

3.4. Interactions of glucose with sphingolipid metabolism

We next sought to confirm the surprising indication from our initial screen that glucose might reduce ceramide accumulation (Figure 1). This was predominately accounted for by a decrease in the most abundant species containing C24:1, and especially C16:0, side-chains (Figure 7A). We reasoned that the most obvious mechanism to explain this reduction would be a mass action effect of glucose, acting as a co-factor for the glycosylation of ceramide catalyzed by glucosylceramide synthase (see Figure 7E). Consistent with this possibility, the ratio of MHC to ceramide was enhanced by glucose stimulation in both islets (Figure 7B) and MIN6 cells (Figure 7C). Surprisingly, another possible mechanism was suggested by analysis
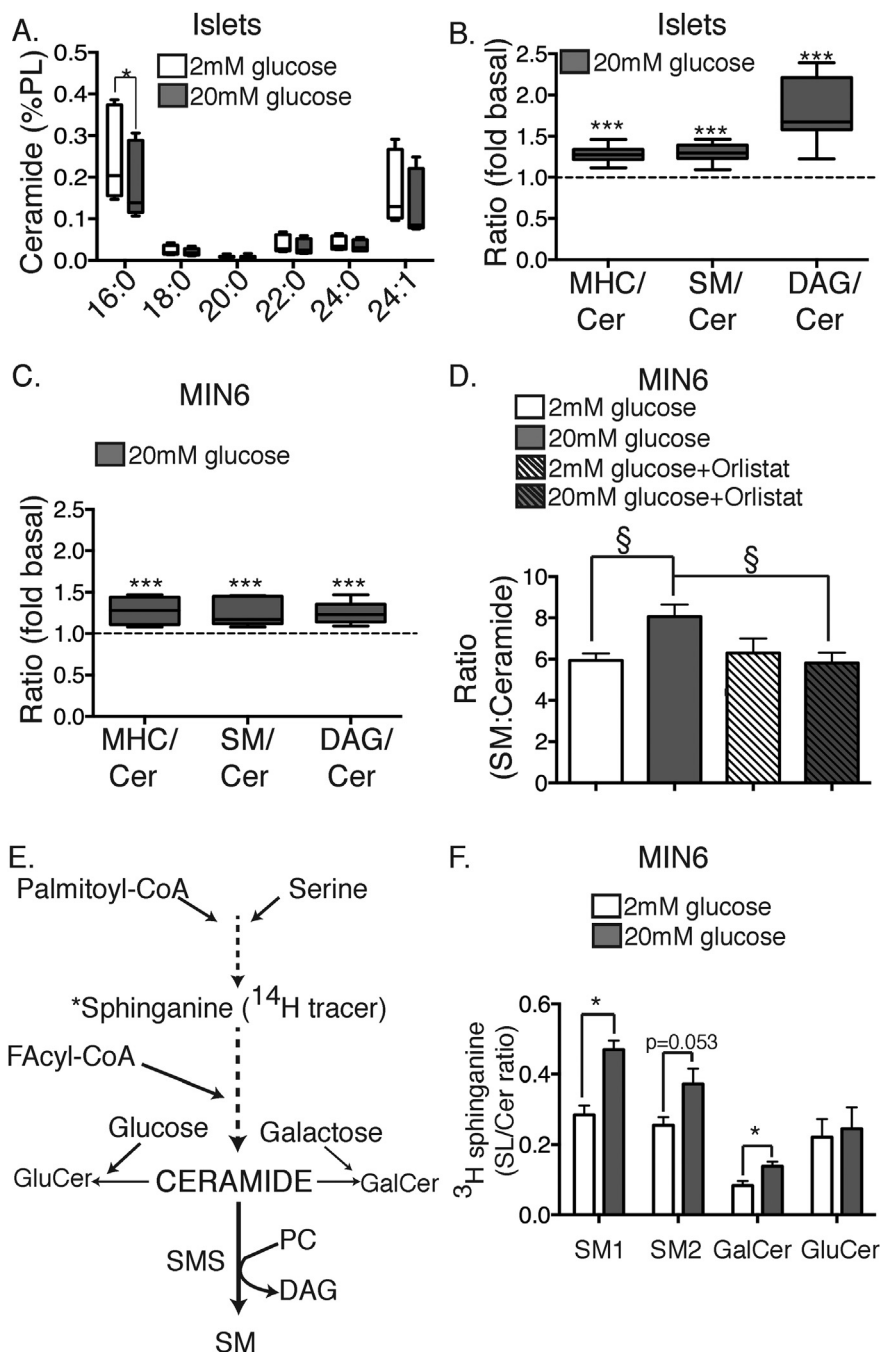
Figure 7: Glucose stimulates the flux of ceramide into SM and GalCer in pancreatic β-cells. Islets (A, B) or MIN6 cells (C, D, F) were stimulated with either 2 mM (white bars), or 20 mM glucose (grey bars) or 2 mM (white striped bars) or 20 mM glucose + 0.2 mM Orlistat (grey striped bars) for 1 h. Total cellular lipids were extracted and then subjected MS (A—D), as per Methods, n = 4—6 MIN6 cells, n = 7—9 islets. (A) ceramide species abundance in isolated islets. Ratio of MHC, SM and DAG to ceramide in islets (B) or MIN6 cells (C) expressed as fold increase at 20 mM versus 2 mM glucose. (D) ratio of SM to ceramide in MIN6 cells in presence or absence of Orlistat. (E) Labelling diagram for incorporation of ^{3}H-sphinganine into sphingolipid pathways, with abbreviations as per text. (F) MIN6 cells were labelled for 1 h with ^{3}H-sphinganine, in the presence of 2 mM (white bars) or 20 mM glucose (grey bars) for 1 h. Cells were then lysed, lipids extracted and separated by TLC analysis and radioactivity of SM, GalCer, ceramide and GluCer determined. Results are expressed as ratios relative to ceramide (n = 4—5). *p < 0.05, **p < 0.01, ***p < 0.001, Student's unpaired t-test; §p < 0.05 one-way ANOVA corrected for multiple comparisons (Sidak).

of the conversion of ceramide to SM, a reaction catalyzed by SMS, which also consumes PC and generates DAG (see Figure 7E). We assessed this step by calculating the ratios of DAG:Cer and SM:Cer, both of which were elevated by glucose stimulation in islets (Figure 7B) and MIN6 cells (Figure 7C). The increment in the SM:Cer ratio due to glucose was completely abolished in the presence of Orlistat (Figure 7D). A possible explanation for this observation is that, by promoting accumulation of DAG, Orlistat causes a feedback inhibition of SM synthesis, consistent with an established function of the DAG activated protein kinase D (PKD) [37,38].

To complement these steady-state analyses we also examined flux through the *de novo* pathways of sphingolipid synthesis using MIN6 cells acutely labelled with ^{3}H-sphinganine (Figure 7F). Glucose enhanced the SM:ceramide ratio for SM containing both long chain (SM1) and, to a lesser extent, very long chain FAs (SM2). We also observed a significant increase in the ratio of GalCer to ceramide, but surprisingly not of GluCer to ceramide (Figure 7F). Thus, in addition to a putative activation of SMS, glucose selectively stimulates the metabolism of ceramide to GalCer (see Figure 7E). Collectively, these results provide the first evidence that glucose acutely regulates sphingolipid metabolism in β-cells, by enhancing the conversion of ceramide into GalCer and especially SM.

3.5. Phospholipid turnover

None of the major phospholipid classes were altered by glucose (Supplementary Table 1 and Figure 1) although there were tendencies towards increases in some of the low abundance, polyunsaturated forms of PC (36:6, 37:5, 38:7, and 40:8) and to a lesser extent PE (38:3). In contrast, there was a consistent decrease in total PC(P) plamalogens (Figure 1). Upon further investigation of both islets (Figure 8A) and MIN6 cells (Figure 8B), we determined that these alterations were most apparent in species with poly-unsaturated side-chains. Indeed, it is known that FAs such as 20:4, 22:5 and 22:6 are particularly enriched in plasmalogens, where they are relatively protected against oxidation by the proximity of the vinyl-ether linkage, which presents itself as an alternative target [39]. In contrast, we found no changes in PE plasmalogens, which are much more abundant than those of PC. Accordingly, in both MIN6 cells and islets, plasmalogens constituted around a third of the total PE pool, versus only 1—2% of overall PC (not shown). This is in similar proportions to that observed in other cell types [39].

4. DISCUSSION

Although it has been recognized for more than 40 years that β-cell lipids are acutely remodelled following glucose stimulation [6], these changes remain poorly defined. Taking advantage of the sensitivity of MS, we have now conducted a characterization of these alterations that we believe is the most comprehensive yet, based both on the total number of species analysed (>350) and the inclusion of members of each of the major classes of sphingolipids, phospholipids, and neutral lipids. Our results highlight alterations in especially in sphingolipid metabolism that have not previously been reported, as well as extend and elaborate prior studies on glycerolipid and plasmalogen turnover. However, we observed no major changes in major phospholipids,

either in overall totals of the different classes (Figure 1) or in individual species thereof (e.g., Supplementary Table 1). This is not to contradict an extensive literature on the hydrolysis of PI and PC in response to glucose [22—25]. Detection of these changes has often required specialized protocols such as analysis of head group markers rather than the associated lipid moieties, shorter stimulation times, and/or tracer approaches for flux estimation. Even so, our strategy did point to elevations in C20:4-containing DAG species, most probably generated by hydrolysis of phospholipids. These increases were most pronounced in the presence of Orlistat. This suggests that DAG liberated by phospholipases is degraded by a neutral lipase, such as DAG lipase, in addition to conversion to phosphatidic acid via the DAG kinase route and re-incorporation into PI. This is consistent with previous studies on the role of DAG lipase in β-cells [23,40].

There is also prior evidence that glucose can activate PLA2 in β-cells to generate the C20:4 FA, arachidonic acid [28]. However, we observed no changes in the lysophospholipids that would be co-generated by this route, particularly lyso-PE. Again, this is probably explained by our use of protocols that were not specifically designed to address this pathway. We did, however, find decreases in polyunsaturated PC(P) species. Previous studies of plamalogens in β-cells have focused on the much more abundant PE forms, with evidence based on tracer protocols of a decrease in some C20:4-containing species in response to prolonged glucose challenge [29,41]. No changes in response to glucose stimulation have been reported previously. One explanation for the reduction in PC(P) species we observe would be their degradation in response to the activation of PLA2. Indeed, there is *in vitro* evidence that the glucose-stimulated form of PLA2 present in β-cells prefers PE plasmalogens as a substrate, compared to PE itself, but this has not been shown for the PC plasmalogens [29]. Another possibility is that the PC(P) species are being converted to the corresponding PC metabolites by breakdown of the vinyl ether linkage. This would be consistent with studies suggesting that reactive oxygen species are generated in the process of glucose-stimulated insulin secretion [42]. It is noteworthy that the polyunsaturated FAs (20:4, 20:5 and 20:6), which characterized the glucose-sensitive PC(P)s in our study, are known to be enriched in both secretory granules and mitochondria in β-cells, where their presence in plasmalogens would seem likely [43]. If so, the possibility that a subpool of polyunsaturated PC(P) at these sites might either participate directly in stimulus-secretion coupling, or help protect against ROS generation, is a topic well worthy of future investigation.

A major goal of the current study was to characterize lipid metabolism downstream of TAG hydrolysis in β-cells, which despite its potential importance in regulating GSIS [11—13], is less well understood than in
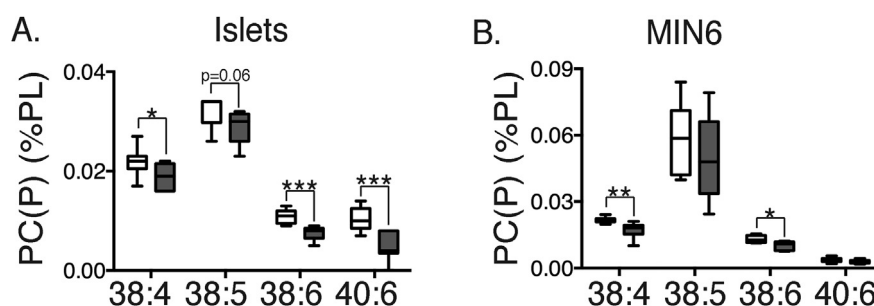

Figure 8: Glucose decreases polyunsaturated PC plasmalogen species. Isolated mouse islets (A) or MIN6 cells (B) were stimulated with either 2 mM (white bars), or 20 mM glucose (grey bars) for 1 h. Total cellular lipids were extracted and then subjected to MS, as per Methods. Results are expressed as percent of total major phospholipids. *p < 0.05; **p < 0.01; ***p < 0.001 Student's unpaired t-test corrected for multiple comparisons (Holm Sidak); n = 8—9 experiments (A) or 6—8 experiments (B).

other tissues. Although it has also been established that glucose stimulates overall lipolysis in β-cells [10,13,17], the regulated step and the overall consequences in terms of lipid metabolism have not been clearly elucidated. We have now shown that di-saturated DAG species were regulated by glucose somewhat differently from other DAG types. These appeared to be derived predominately from TAG hydrolysis, as witnessed by an absolute sensitivity to Orlistat. Investigation of product:precursor relationships further suggested that this generation of di-saturated DAGs from TAG was specifically stimulated by glucose. All in all, this would be consistent with an activation of ATGL [18,19] and probably explains earlier observations of a relative enrichment of saturated FAs in DAG of glucose-stimulated β-cells, even though the exact DAG species were not identified [22,23]. Although di-saturated DAGs were the most obvious products of glucose stimulated TAG hydrolysis, others such as the highly abundant 16:0_18:1 DAG species were also generated in this manner (Figure 4B). We propose that the di-saturated DAGs (more specifically those containing C16:0 side-chains) are nevertheless an excellent marker for TAG hydrolysis (at least under standard culture conditions) because they are predominantly generated via this route in response to glucose, even though they are not very abundant. In contrast, 16:0_18:1 DAG is very likely one of the major species released by TAG hydrolysis in quantitative terms, but it is almost certainly generated by additional means such as de novo synthesis [3,8]. Against this baseline, the contribution of TAG hydrolysis is thus less obvious in the product:precursor analysis. As a caveat, however, we would add that a definitive quantification of the relative contributions of all of these competing routes would require specific genetic intervention at key control points, in conjunction with more sophisticated MS protocols combining flux and mass measurements.

Our studies further demonstrated that glucose elevated 18:1 MAG in MIN6 cells, but not other MAG species, and that this was most probably derived from 18:1-containing DAGs generated via TAG hydrolysis. Indeed, ATGL activation appears to be the flux-generating step for the overall pathway, since the product:precursor analyses did not suggest that the conversion of DAG to MAG was independently modulated by glucose. This is an important observation because HSL, which catalyzes this conversion, is highly regulated in other tissues [44] but its relevance to GSIS in β-cells has been difficult to interpret [10,13,15]. Addressing the mechanism of activation of ATGL by glucose should now be a focus for future studies.

Our chief aim was to characterize lipid metabolism rather than signalling. As such, we have focused on a single time point (1 h) and only compared responses at basal versus maximal glucose stimulation. However, it seems probable that our findings might have some potential relevance to the regulation of GSIS. We believe that DAGs generated by ATGL are unlikely to be important as signalling intermediates because they do not possess the correct side-chain configuration to interact with effector proteins such as protein kinases [18,19]. Rather, we suggest that the more likely role of ATGL activation by glucose is the generation of 16:0_18:1 DAG, which serves as the precursor for the generation of 18:1 MAG via an Orlistat-sensitive lipase. Importantly, this MAG species has been previously shown to stimulate insulin secretion [45,46]. Our findings are also compatible with another recent study implicating MAG in the regulation of GSIS, although, in that instance, the focus was on saturated MAG species, which appear to interact with the signalling molecule Munc13-1 [35]. We certainly wouldn't discount a role for these saturated MAGs, although they were relatively minor species in our protocol whereby lipids were analysed directly using MS. In contrast, Zhao et al. isolated MAGs via a multi-step approach entailing TLC, saponification and reverse phase HPLC. Using multiple reaction monitoring we further

established that 95% of overall MAG mass was contributed by only 5 individual species, of which 18:1 MAG was the most abundant. We would maintain that MS is inherently more accurate for relative quantification of individual species characterized by different side-chains, although it can not distinguish the exact configuration of those side-chains. Thus, if glucose only stimulated formation of one or other of the 1-MAG or 2-MAG isomers, as might be the case [36], our analysis would underestimate the size of the increase, potentially explaining why we detected no obvious changes at all in di-saturated MAGs, and why the augmentation of 18:1 MAG reached statistical significance only in MIN6 cells. Finally, the major focus of the previous studies was on the enzyme α,β-hydrolase domain 6 [35,36], which degrades MAG, whereas we concentrated more specifically on upstream TAG hydrolysis. Perhaps these differences might contribute to the alternative emphases on 18:1 MAG versus the saturated species, but this would need to be resolved by future investigations.

Finally, our analyses revealed an unexpected impact of glucose on sphingolipid metabolism in β-cells. We observed a highly reproducible decrease in total ceramide that was, however, probably too subtle to have been detected in a prior study using MIN6 cells [47]. This reduction might be partially explained by an inhibition of de novo synthesis due to a previously documented depletion in palmitoyl CoA under these conditions [3]. However, our results also highlight an enhanced flux of ceramide into SM and GalCer, which was demonstrated directly. No overall change in SM mass was detected, probably implicating changes in ceramide or SM at restricted sites within the cell. While these changes might themselves have functional effects, for example by modulating lipid rafts [32], an alternative interpretation would be that they reflect localized activation of SMS. This enzyme has important but poorly understood roles in β-cells in regulating the formation of secretory granules, and downstream exocytosis [26,27]. In this context the key event is localized generation of DAG, formed concomitantly with SM via SMS, and which activates PKD [27,48,49]. Both product:precursor and flux analyses from our study are at least consistent with the idea that localized increases in DAG might be generated via this route during glucose stimulation. Using tracer techniques that, unlike MS, allow the resolution of MHC into different entities depending on the type of hexose incorporated, we further showed that glucose regulates the synthesis of GalCer. Surprisingly, this was not the case for GluCer, as might have been expected simply by mass action. The physiological relevance of this new observation might have to do with repletion of sulfatide, a downstream metabolite of GalCer that has been implicated in the maintenance of proinsulin reserves and secretory granule content [50]. Obviously, further studies will be required to extend these novel findings that glucose regulates sphingolipid metabolism in β-cells.

ACKNOWLEDGEMENTS

CONFLICT OF INTEREST

None declared.

APPENDIX A. SUPPLEMENTARY DATA

Supplementary data related to this article can be found at http://dx.doi.org/10.1016/j.molmet.2016.04.003.

REFERENCES

[1] Ashcroft, F.M., Rorsman, P., 2012. Diabetes mellitus and the beta cell: the last ten years. Cell 148:1160—1171.

[2] Huang, M., Joseph, J.W., 2014. Assessment of the metabolic pathways associated with glucose-stimulated biphasic insulin secretion. Endocrinology 155:1653—1666.

[3] Lorenz, M.A., El Azzouny, M.A., Kennedy, R.T., Burant, C.F., 2013. Metabolome response to glucose in the β-cell line INS-1 832/13. Journal of Biological Chemistry 288:10923—10935.

[4] Spegel, P., Sharoyko, V.V., Goehring, I., Danielsson, A.P.H., Malmgren, S., Nagorny, C.L.F., et al., 2013. Time-resolved metabolomics analysis of beta-cells implicates the pentose phosphate pathway in the control of insulin release. Biochemical Journal 450:595—605.

[5] Berne, C., 1975. Metabolism of lipids in mouse pancreatic-islets - oxidation of fatty-acids and ketone-bodies. Biochemical Journal 152:661—666.

[6] Berne, C., 1975. Metabolism of lipids in mouse pancreatic-islets - biosynthesis of triacylglycerols and phospholipids. Biochemical Journal 152:667—673.

[7] Corkey, B.E., Glennon, M.C., Chen, K.S., Deeney, J.T., Matschinsky, F.M., Prentki, M., 1989. A role for malonyl-CoA in glucose-stimulated insulin secretion from clonal pancreatic beta-cells. Journal of Biological Chemistry 264:21608—21612.

[8] MacDonald, M.J., Dobrzyn, A., Ntambi, J., Stoker, S.W., 2008. The role of rapid lipogenesis in insulin secretion: insulin secretagogues acutely alter lipid composition of INS-1 832/13 cells. Archives of Biochemistry and Biophysics 470:153—162.

[9] Mulder, H., Yang, S., Winzell, M.S., Holm, C., Ahren, B., 2004. Inhibition of lipase activity and lipolysis in rat islets reduces insulin secretion. Diabetes 53:122—128.

[10] Peyot, M.L., Nolan, C.J., Soni, K., Joly, E., Lussier, R., Corkey, B.E., et al., 2004. Hormone-sensitive lipase has a role in lipid signaling for insulin secretion but is nonessential for the incretin action of glucagon-like peptide 1. Diabetes 53:1733—1742.

[11] Corkey, B.E., Deeney, J.T., Yaney, G.C., Tornheim, K., Prentki, M., 2000. The role of long-chain fatty acyl-CoA esters in beta-cell signal transduction. Journal of Nutrition 130:299S—304S.

[12] Nolan, C.J., Madiraju, M.S., Delghingaro-Augusto, V., Peyot, M.L., Prentki, M., 2006. Fatty acid signaling in the β-cell and insulin secretion. Diabetes 55(Suppl. 2):S16—S23.

[13] Fex, M., Mulder, H., 2008. Lipases in the pancreatic beta-cell: implications for insulin secretion. Biochemical Society Transactions 36:885—890.

[14] Masiello, P., Novelli, M., Bombara, M., Fierabracci, V., Vittorini, S., Prentki, M., et al., 2002. The antilipolytic agent 3,5-dimethylpyrazole inhibits insulin release in response to both nutrient secretagogues and cyclic adenosine monophosphate agonists in isolated rat islets. Metabolism 51:110—114.

[15] Fex, M., Haemmerle, G., Wierup, N., Dekker-Nitert, M., Rehn, M., Ristow, M., et al., 2009. A beta cell-specific knockout of hormone-sensitive lipase in mice results in hyperglycaemia and disruption of exocytosis. Diabetologia 52:271—280.

[16] Roduit, R., Masiello, P., Wang, S.P., Li, H., Mitchell, G.A., Prentki, M., 2001. A role for hormone-sensitive lipase in glucose-stimulated insulin secretion: a study in hormone-sensitive lipase-deficient mice. Diabetes 50:1970—1975.

[17] Peyot, M.L., Guay, C., Latour, M.G., Lamontagne, J., Lussier, R., Pineda, M., et al., 2009. Adipose triglyceride lipase is implicated in fuel- and non-fuel-stimulated insulin secretion. Journal of Biological Chemistry 284:16848—16859.

[18] Eichmann, T.O., Kumari, M., Haas, J.T., Farese Jr., R.V., Zimmermann, R., Lass, A., et al., 2012. Studies on the substrate and stereo/regioselectivity of adipose triglyceride lipase, hormone-sensitive lipase, and diacylglycerol-O-acyltransferases. Journal of Biological Chemistry 287:41446—41457.

[19] Zechner, R., Zimmermann, R., Eichmann, T.O., Kohlwein, S.D., Haemmerle, G., Lass, A., et al., 2012. FAT SIGNALS—lipases and lipolysis in lipid metabolism and signaling. Cell Metabolism 15:279—291.

[20] Singh, R., Kaushik, S., Wang, Y., Xiang, Y., Novak, I., Komatsu, M., et al., 2009. Autophagy regulates lipid metabolism. Nature 458:1131—1135.

[21] Pearson, G.L., Mellet, N., Chu, K.Y., Cantley, J., Davenport, A., Bourbon, P., et al., 2014. Lysosomal acid lipase and lipophagy are constitutive negative regulators of glucose-stimulated insulin secretion from pancreatic beta cells. Diabetologia 57:129—139.

[22] Peter-Riesch, B., Fathi, M., Schlegel, W., Wollheim, C.B., 1988. Glucose and carbachol generate 1,2-diacylglycerols by different mechanisms in pancreatic islets. Journal of Clinical Investigation 81:1154—1161.

[23] Wolf, B.A., Easom, R.A., Hughes, J.H., McDaniel, M.L., Turk, J., 1989. Secretagogue-induced diacylglycerol accumulation in isolated pancreatic islets. Mass spectrometric characterization of the fatty acyl content indicates multiple mechanisms of generation. Biochemistry 28:4291—4301.

[24] Biden, T.J., Peter-Riesch, B., Schlegel, W., Wollheim, C.B., 1987. Ca2+-mediated generation of inositol 1,4,5-triphosphate and inositol 1,3,4,5-tetrakisphosphate in pancreatic islets. Studies with K+, glucose, and carbamylcholine. Journal of Biological Chemistry 262:3567—3571.

[25] Hughes, W.E., Elgundi, Z., Huang, P., Frohman, M.A., Biden, T.J., 2004. Phospholipase D1 regulates secretagogue-stimulated insulin release in pancreatic beta-cells. Journal of Biological Chemistry 279:27534—27541.

[26] Boslem, E., Meikle, P.J., Biden, T.J., 2012. Roles of ceramide and sphingolipids in pancreatic β-cell function and dysfunction. Islets 4:177—187.

[27] Subathra, M., Qureshi, A., Luberto, C., 2011. Sphingomyelin synthases regulate protein trafficking and secretion. PLoS One 6:e23644.

[28] Ramanadham, S., Ali, T., Ashley, J.W., Bone, R.N., Hancock, W.D., Lei, X., 2015. Calcium-independent phospholipases A2 and their roles in biological processes and diseases. Journal of Lipid Research 56:1643—1668.

[29] Ramanadham, S., Bohrer, A., Mueller, M., Jett, P., Gross, R.W., Turk, J., 1993. Mass spectrometric identification and quantitation of arachidonate-containing phospholipids in pancreatic islets: prominence of plasmenylethanolamine molecular species. Biochemistry 32:5339—5351.

[30] Boslem, E., MacIntosh, G., Preston, A.M., Bartley, C., Busch, A.K., Fuller, M., et al., 2011. A lipidomic screen of palmitate-treated MIN6 β-cells links sphingolipid metabolites with endoplasmic reticulum (ER) stress and impaired protein trafficking. Biochemical Journal 435:267—276.

[31] Weir, J.M., Wong, G., Barlow, C.K., Greeve, M.A., Kowalczyk, A., Almasy, L., et al., 2013. Plasma lipid profiling in a large population-based cohort. Journal of Lipid Research 54:2898—2908.

[32] Boslem, E., Weir, J.M., Macintosh, G., Sue, N., Cantley, J., Meikle, P.J., et al., 2013. Alteration of endoplasmic reticulum lipid rafts contributes to lipotoxicity in pancreatic β-cells. Journal of Biological Chemistry 288:26569—26582.

[33] Meikle, P.J., Wong, G., Tsorotes, D., Barlow, C.K., Weir, J.M., Christopher, M.J., et al., 2011. Plasma lipidomic analysis of stable and unstable coronary artery disease. Arteriosclerosis, Thrombosis, and Vascular Biology 31:2723—2732.

[34] Lavie, Y., Cao, H., Bursten, S.L., Giuliano, A.E., Cabot, M.C., 1996. Accumulation of glucosylceramides in multidrug-resistant cancer cells. Journal of Biological Chemistry 271:19530—19536.

[35] Zhao, S., Mugabo, Y., Iglesias, J., Xie, L., Delghingaro-Augusto, V., Lussier, R., et al., 2014. α/β-Hydrolase domain-6-accessible monoacylglycerol controls glucose-stimulated insulin secretion. Cell Metabolism 19:993—1007.

[36] Zhao, S., Pourshariffi, P., Mugabo, Y., Levens, E.J., Vivot, K., Attane, C., et al., 2015. α/β-Hydrolase domain-6 and saturated long chain monoacylglycerol regulate insulin secretion promoted by both fuel and non-fuel stimuli. Molecular Metabolism 4:940—950.

[37] Fu, Y., Rubin, C.S., 2011. Protein kinase D: coupling extracellular stimuli to the regulation of cell physiology. EMBO Reports 12:785—796.

Original article

[38] Fugmann, T., Hausser, A., Schoffler, P., Schmid, S., Pfizenmaier, K., Olayioye, M.A., 2007. Regulation of secretory transport by protein kinase D-mediated phosphorylation of the ceramide transfer protein. Journal of Cell Biology 178:15—22.

[39] Wallner, S., Schmitz, G., 2011. Plasmalogens the neglected regulatory and scavenging lipid species. Chemistry and Physics of Lipids 164:573—589.

[40] Konrad, R.J., Major, C.D., Wolf, B.A., 1994. Diacylglycerol hydrolysis to arachidonic acid is necessary for insulin secretion from isolated pancreatic islets: sequential actions of diacylglycerol and monoacylglycerol lipases. Biochemistry 33:13284—13294.

[41] Ramanadham, S., Bohrer, A., Gross, R.W., Turk, J., 1993. Mass spectrometric characterization of arachidonate-containing plasmalogens in human pancreatic islets and in rat islet beta-cells and subcellular membranes. Biochemistry 32:13499—13509.

[42] Pi, J., Bai, Y., Zhang, Q., Wong, V., Floering, L.M., Daniel, K., et al., 2007. Reactive oxygen species as a signal in glucose-stimulated insulin secretion. Diabetes 56:1783—1791.

[43] MacDonald, M.J., Ade, L., Ntambi, J.M., Ansari, I.U., Stoker, S.W., 2015. Characterization of phospholipids in insulin secretory granules and mitochondria in pancreatic beta cells and their changes with glucose stimulation. Journal of Biological Chemistry 290:11075—11092.

[44] Coleman, R.A., Mashek, D.G., 2011. Mammalian triacylglycerol metabolism: synthesis, lipolysis, and signaling. Chemical Reviews 111:6359—6386.

[45] Saadeh, M., Ferrante, T.C., Kane, A., Shirihai, O., Corkey, B.E., Deeney, J.T., 2012. Reactive oxygen species stimulate insulin secretion in rat pancreatic islets: studies using mono-oleoyl-glycerol. PLoS One 7:e30200.

[46] Zawalich, W.S., Zawalich, K.C., Rasmussen, H., 1989. The effect of mono-oleoylglycerol on insulin secretion from isolated perifused rat islets. Diabetologia 32:360—364.

[47] Cantrell Stanford, J., Morris, A.J., Sunkara, M., Popa, G.J., Larson, K.L., Ozcan, S., 2012. Sphingosine 1-phosphate (S1P) regulates glucose-stimulated insulin secretion in pancreatic beta cells. Journal of Biological Chemistry 287: 13457—13464.

[48] Gehart, H., Goginashvili, A., Beck, R., Morvan, J., Erbs, E., Formentini, I., et al., 2012. The BAR domain protein Arfaptin-1 controls secretory granule biogenesis at the trans-Golgi network. Developmental Cell 23:756—768.

[49] Sumara, G., Formentini, I., Collins, S., Sumara, I., Windak, R., Bodenmiller, B., et al., 2009. Regulation of PKD by the MAPK p38δ in insulin secretion and glucose homeostasis. Cell 136:235—248.

[50] Buschard, K., Blomqvist, M., Osterbye, T., Fredman, P., 2005. Involvement of sulfatide in beta cells and type 1 and type 2 diabetes. Diabetologia 48:1957—1962.